

β -Limit Investigation in a Straight Stellarator using NIMROD

Mark Schlutt, Chris C. Hegna, and Carl R. Sovinec
University of Wisconsin

Eric D. Held
Utah State University

Scott E. Kruger
Tech-X Corporation



Thursday, November 11, 2010

Motivation - 3D magnetic field structure may be related to higher achievable β .

- **Recent work indicates that in stellarators, stability may not limit β . Instead β may be limited by equilibrium physics.**^{1 2}
_{3 4}
 - What maximum β is possible?
 - What factors and physics limit achievable β ?
 - What equilibrium characteristics limit β ?
- **The magnetic topology appears to change to limit β ; flux surfaces deteriorate, enhancing transport.**
 - Pressure-induced currents may degrade magnetic surface integrity.
 - "Weakly stochastic" edge magnetic fields are produced, possibly as a result of self-consistent transport physics.

¹M. Hirsch, et al., Plasma Phys. Control. Fusion, **50**, 1(2008).

²M. Sato, et al., 2008 IAEA Proceedings.

³A. Reiman, et al., Nucl. Fusion, **47**,572(2007)

⁴M.C. Zarnstorff, et al., 2004 IAEA Fusion Energy Conference.

Motivation - Answering these questions is NOT trivial.

- **Calculating the structure of finite- β 3D magnetic equilibria is not straightforward.**
 - Good flux surfaces are not guaranteed to exist in 3D configurations.
 - The equations of MHD equilibrium do not allow for stochastic regions to support a pressure gradient: $\mathbf{B} \cdot \nabla p = 0$.
 - Notions of equilibrium and stability become blurred.
 - For example, in a resistive MHD model, *equilibrium* island widths depend on parameters related to *stability*.
- **As β increases, the magnetic topology changes.**

⇒ This motivates using a time-dependent extended MHD code to model the 3D equilibrium.

NIMROD is used to study the finite- β response of these equilibria.

1. Vacuum field is **helically symmetric**.

- Finite- β equilibria created by heating, with anisotropic conduction:
 $\chi_{\parallel}/\chi_{\perp} = 10^6$.
- Stability properties are investigated by perturbing the system:
 - A shear Alfvén wave is launched at $t=0$.
 - Many small symmetry-spoiling harmonics are included in the boundary conditions for two time steps. After the first two time steps, the vacuum magnetic field consists of only the dominant harmonic.

2. Vacuum field has **spoiled symmetry**, heated and perturbed same as above.

- Each of these cases is heated with an ad-hoc, volumetric heating source of various strengths \Rightarrow 4 total cases.

The initial helical vacuum equilibrium magnetic field is analytically prescribed in NIMROD.

Solving Laplace's equation in a periodic cylinder yields a scalar potential to describe the helical vacuum magnetic field for a straight stellarator:

$$\mathbf{B} = \nabla\phi$$

$$\phi = B_0 \left[R\zeta + \sum_{m,n \text{ pairs}} \epsilon_{mn} \frac{Rm}{n} I_m \left(\frac{nr}{R} \right) \sin(m\theta - n\zeta) \right]$$

where:

$\epsilon_{mn} = \frac{b_{mn}}{B_0}$ is the relative amplitude of the helical harmonic of the magnetic field.
 $I_m(x)$ is the modified Bessel function of order m and argument x .

Magnetic field structure and spectrum are controlled by choice of ϵ_{mn} :

$$t \simeq \sum_{m,n} \frac{\epsilon_{mn}^2}{4} \left(\frac{m^2 R^2}{n^2 r} \frac{d}{dr} \right)^2 I_m^2 \left(\frac{nr}{R} \right)$$

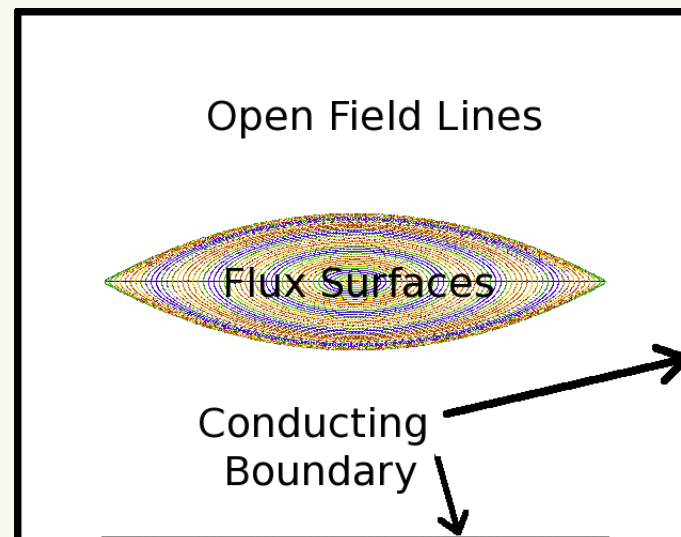
- * Helically symmetric equilibria are a special subclass of solutions
 $\implies \vec{B} = \vec{B}(\psi, M\theta - N\zeta)$

The boundary condition is a line-tied perfectly conducting shell.

- In general 3-D magnetic configurations, field lines intersect the computational boundary.
- After the analytic vacuum equilibrium is prescribed, a line-tied condition is enforced at the boundary. That is, the normal component of the magnetic field at the wall is NOT updated for $t > 0$:

$$\frac{d}{dt} \vec{B} \cdot \hat{n}|_{bdry} = 0$$

This results in a vacuum magnetic field structure which persists in time, despite perturbations to the magnetic field.



Straight Stellarator Parameters and Figures of Merit.

All calculations take place in straight stellarator geometry where:

$a = \text{minor radius} \simeq 0.2\text{m}$
$B_0 = \text{Guide field in axial direction} = 1 \text{ T}$
$T_{bckgrd} = \text{background temperature (at plasma edge)} = 1 \text{ eV}$
$\text{Kinematic viscosity} = 1 \text{ m}^2/\text{s}$
$\text{Electrical Diffusivity } (\eta/\mu_0) = 1 \text{ m}^2/\text{s}$
$\tau_E = \text{Energy confinement time} = 6.9 \cdot 10^{-3} \text{ s}$
$S = \text{Lundquist number} = 175,000$
$V_A = \text{Alfven speed} = 8.8 \cdot 10^5 \text{ m/s}$
$\chi_{\perp} = \text{perpendicular thermal diffusivity} = 1 \text{ m}^2/\text{s}$
$\chi_{\parallel} = \text{parallel thermal diffusivity, varied from} = 10^5 \text{ m}^2/\text{s} \text{ to } 10^6 \text{ m}^2/\text{s}$
$P_m = \text{magnetic Prantdl number} = 1$

The $(m=2, n=2, \epsilon=.85)$ case is studied.

- Core rotational transform: $t(0) = 0.474$.
- Heating for this case is broad - "tent shape" - peak at the center to 0 at LCFS in vacuum at each point in the domain.
- Heating profile rotates with the shape of the plasma: $n=2$.

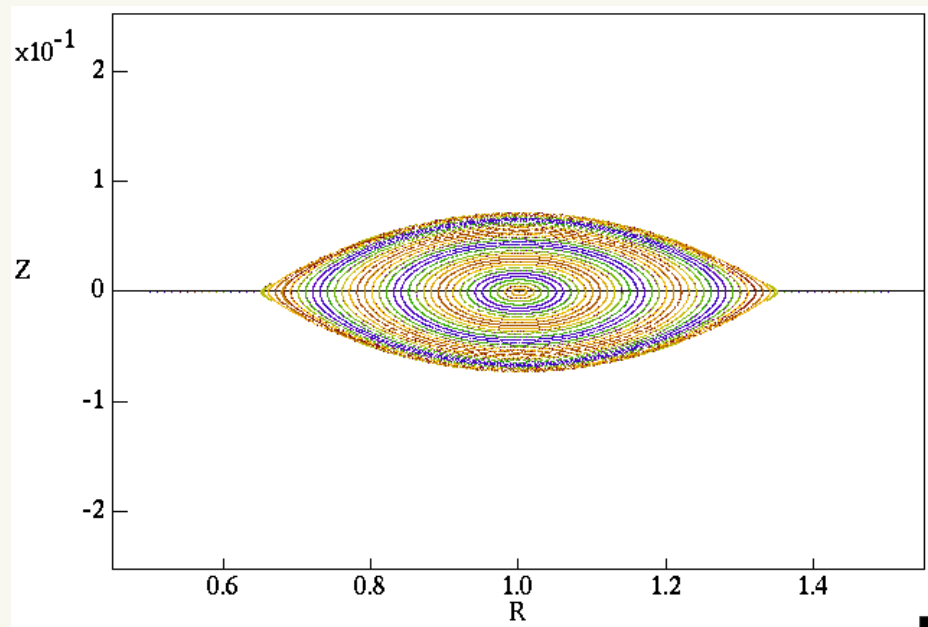


Figure 1: Poincaré plot at $t=0, \zeta = 0$.

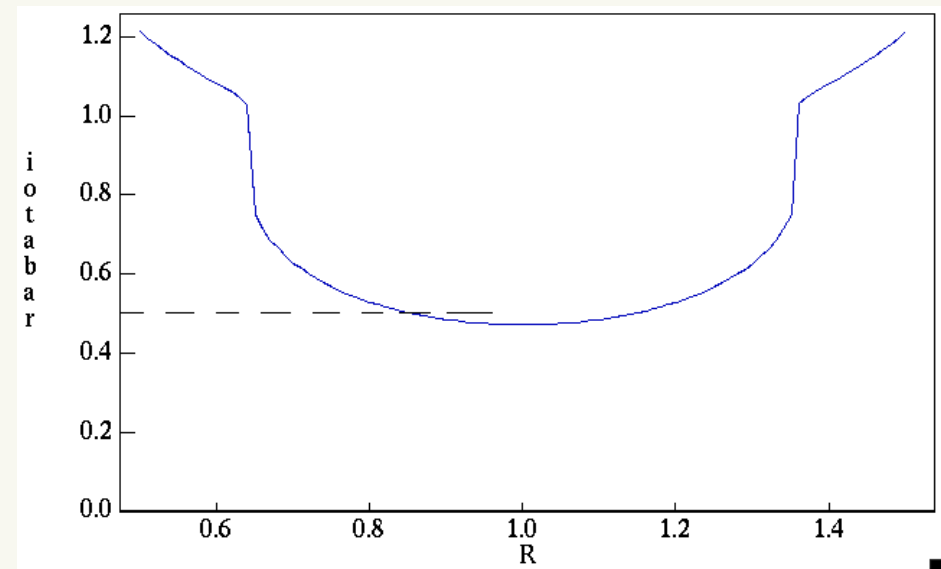


Figure 2: Rotational transform profile at $t=0, \zeta = 0$.

The helically symmetric ($m=2, n=2, \epsilon=.85$) case is perturbed and heated. (Case 1)

Flux surfaces remain largely intact during early heating.

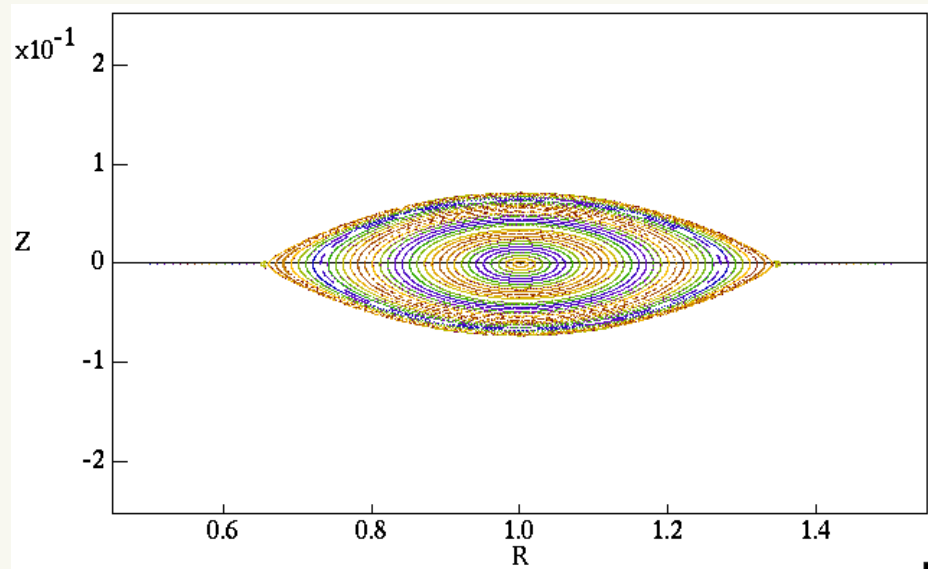


Figure 3: Poincaré plot at $t=2.0 \cdot 10^{-3}$ s, $\zeta = 0$.

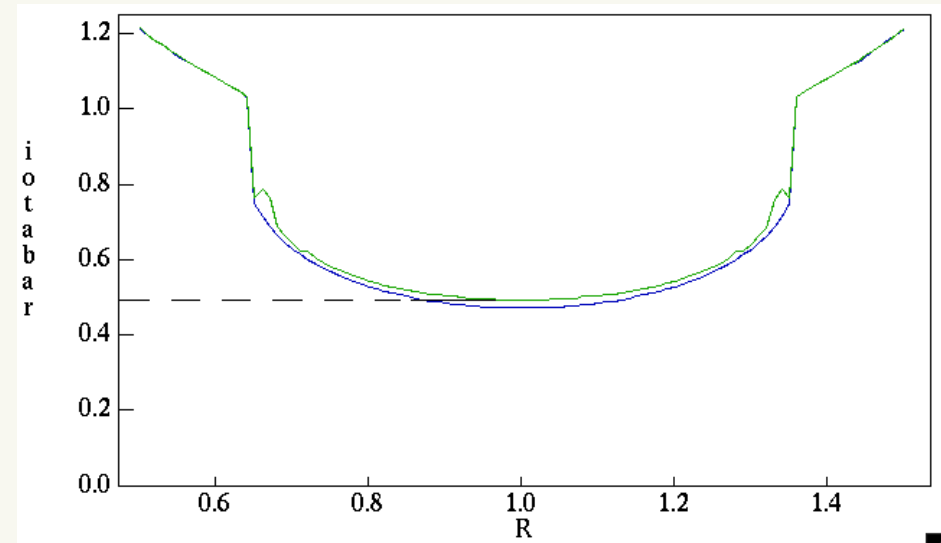


Figure 4: Rotational transform profiles at $t=0$ and $t=6.6 \cdot 10^{-3}$ s.

The helically symmetric ($m=2, n=2, \epsilon=.85$) case is perturbed and heated.

As β is increased, a core mode appears and relaxation occurs.

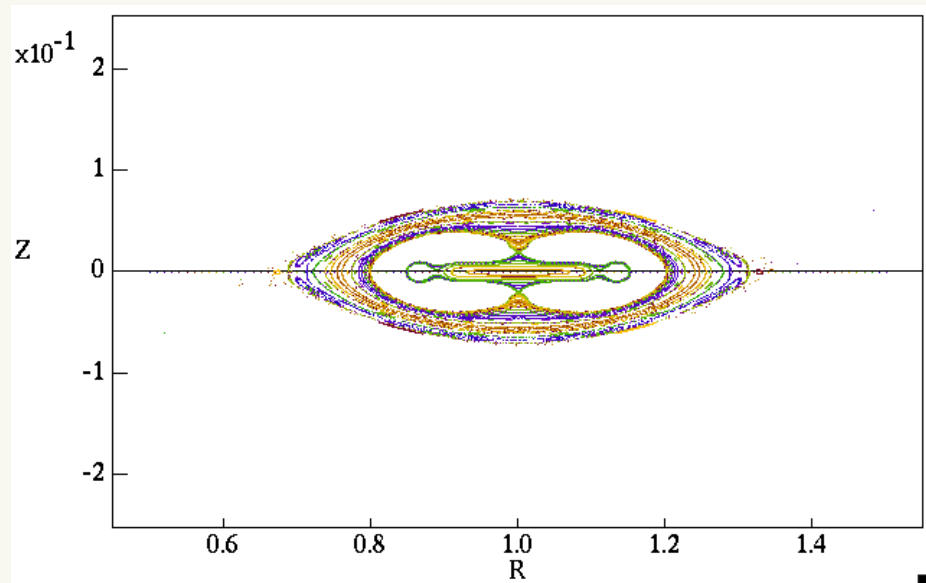


Figure 5: Poincaré plot at $t=6.6 \cdot 10^{-3} \text{ s}$, $\zeta = 0$.

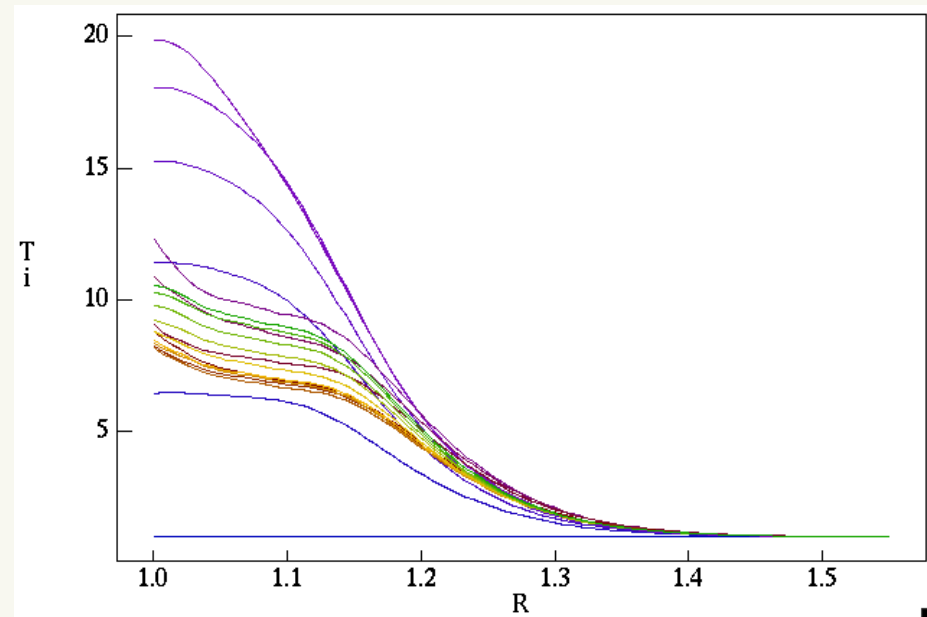


Figure 6: Temperature profile at various times.

The perturbed helically symmetric ($m=2, n=2, \epsilon=.85$) case reaches a maximum β of 1.05%.

$n=1$ and $n=3$ modes are the largest growing modes, with a linear growth rate of $\sim 4500s^{-1} \Rightarrow$ resistive

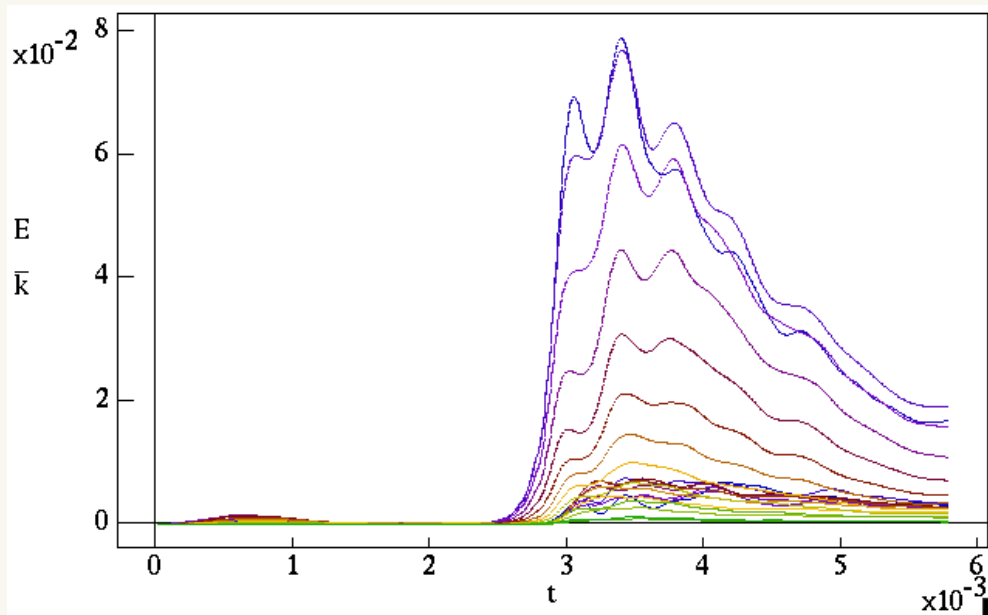


Figure 7: Kinetic energy for all modes.

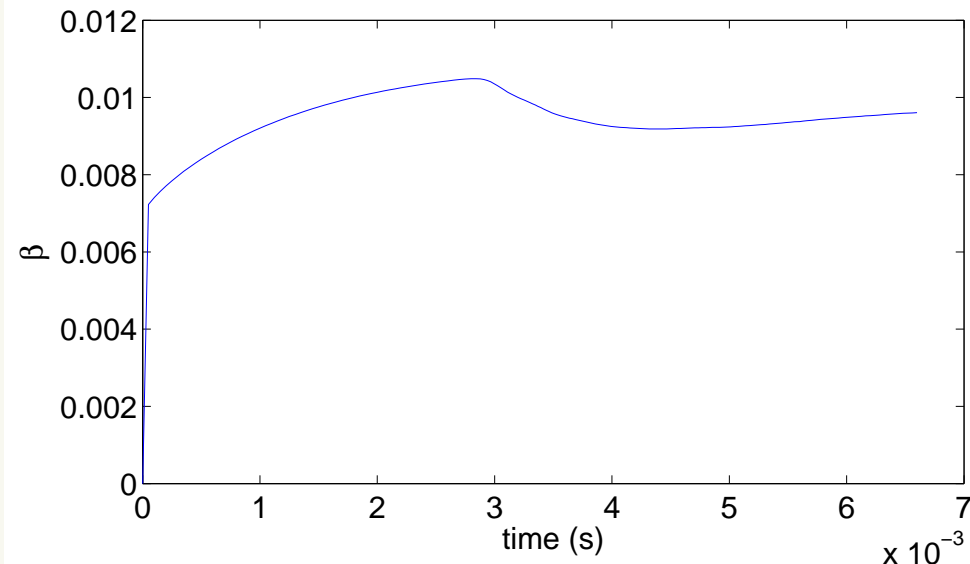


Figure 8: Maximum $\beta=1.05\%$.

The spoiled symmetry ($m=2, n=2, \epsilon=.85$) case is perturbed and heated. (Case 2)

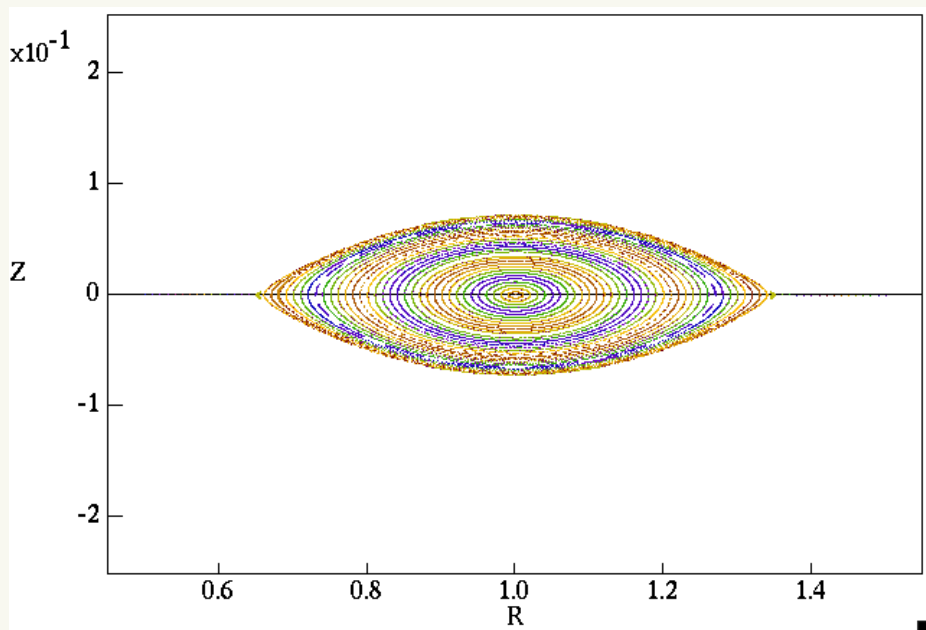


Figure 9: Poincare plot at $t=2.00 \cdot 10^{-3} \text{s}$, $\zeta = 0$.

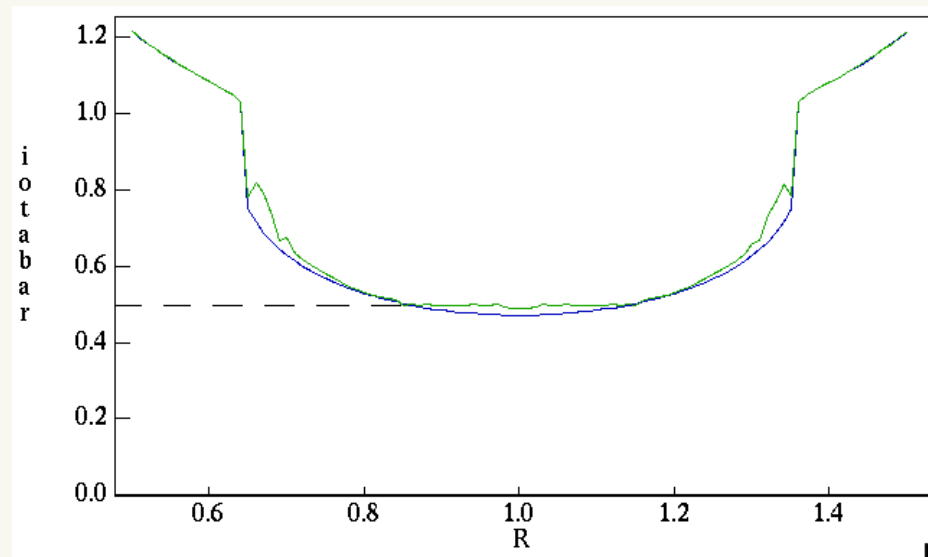


Figure 10: Rotational transform profiles at $t=0$ and $t=4.04 \cdot 10^{-3} \text{s}$.

The spoiled symmetry ($m=2, n=2, \epsilon=.85$) case is perturbed and heated.

Again, as β is increased, relaxation occurs after the development of a core mode.

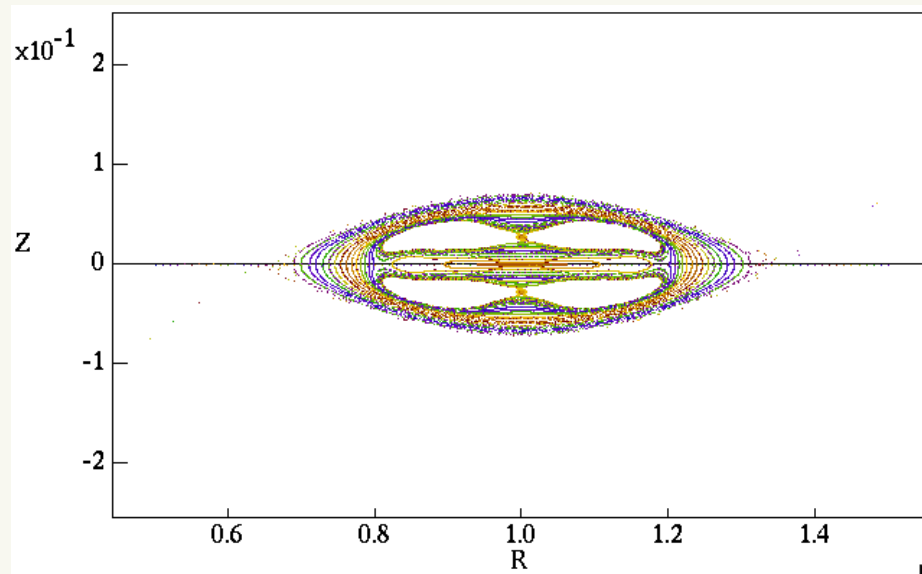


Figure 11: Poincare plot at $t=4.04 \cdot 10^{-3}s$, $\zeta = 0$.

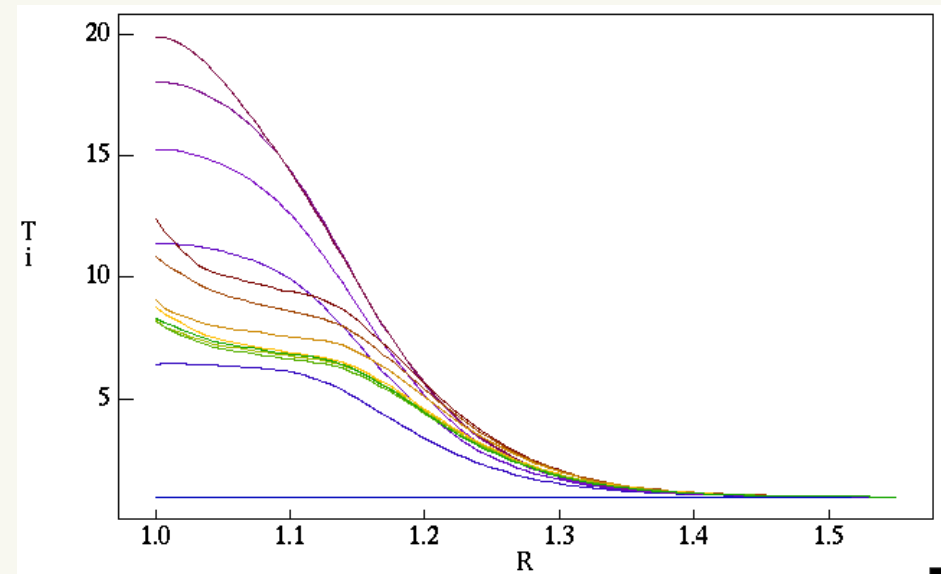


Figure 12: Temperature profile at various times.

The spoiled symmetry ($m=2, n=2, \epsilon=.85$) case reaches a maximum β of 1.05%.

$n=1$ and $n=3$ modes are the largest growing modes, with the same resistive growth rate as previously.

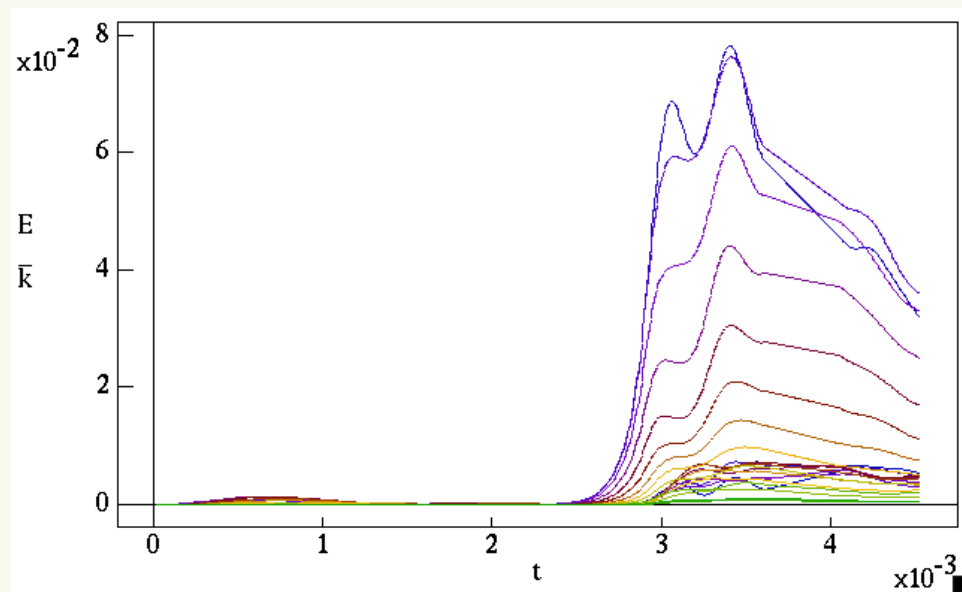


Figure 13: Kinetic energy for all modes.

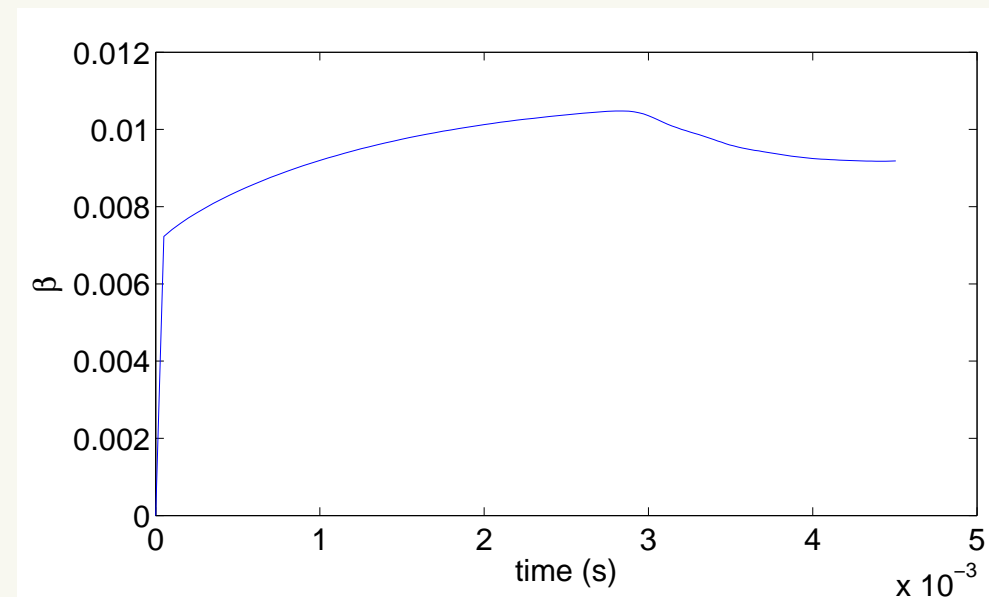


Figure 14: Maximum $\beta=1.05\%$.

The $(m=2, n=2, \epsilon=.75)$ case is studied.

- Core rotational transform: $t(0) = 0.34$.
- Heating for this case is broad - "tent shape" - peak at the center to 0 at LCFS in vacuum for each poloidal plane.
 - Heating is $n=2$. That is, as one travels axially along the cylinder, the heating profile rotates with the shape of the plasma.

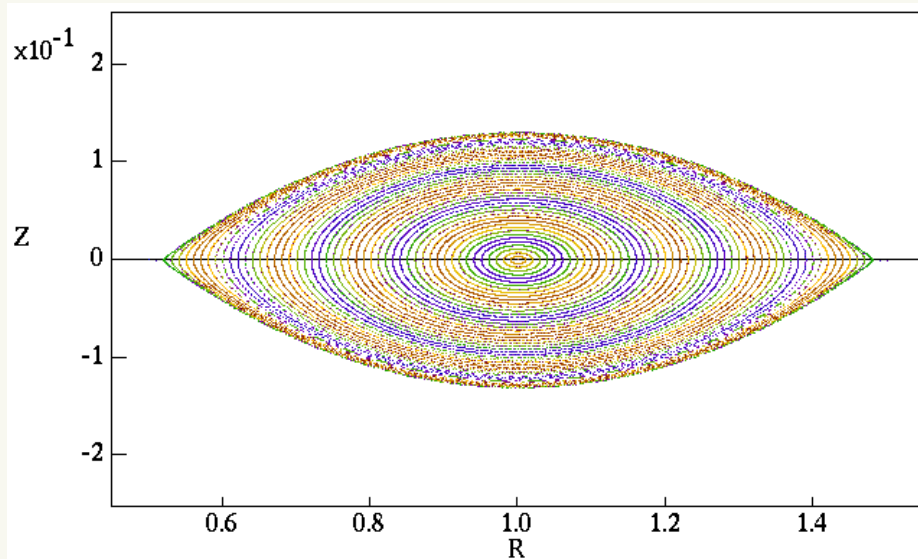


Figure 15: Poincaré plot at $t=0$, $\zeta = 0$.

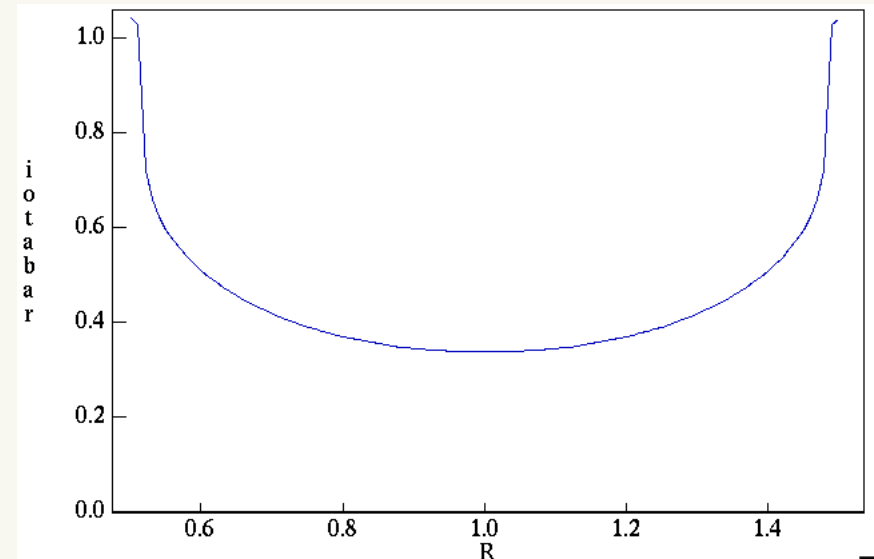


Figure 16: Rotational transform profile at $t=0$, $\zeta = 0$.

The helically symmetric ($m=2, n=2, \epsilon=.75$) case is perturbed and heated. (Case 1).

Flux surfaces remain largely intact with some stochasticity near the edge.

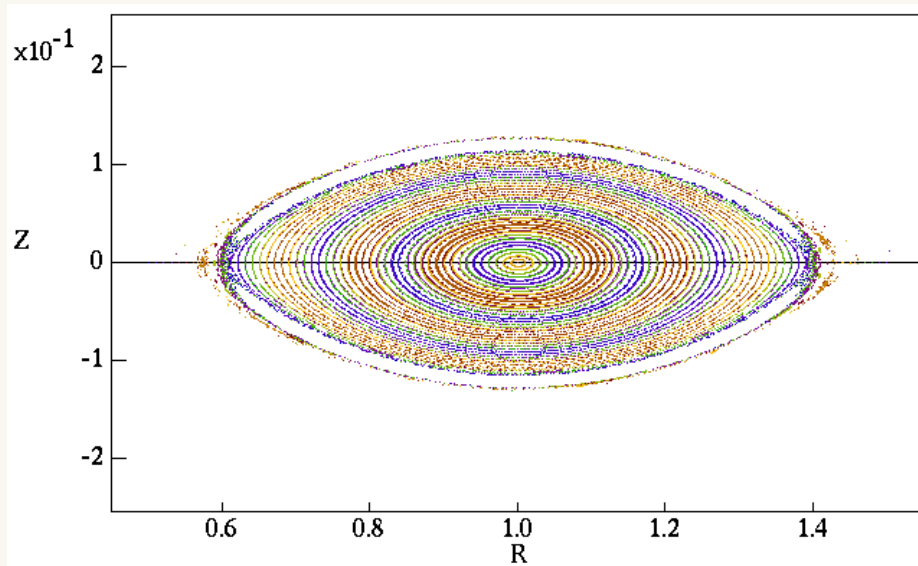


Figure 17: Poincaré plot at $t=4.8 \cdot 10^{-4}$ s, $\zeta = 0$.

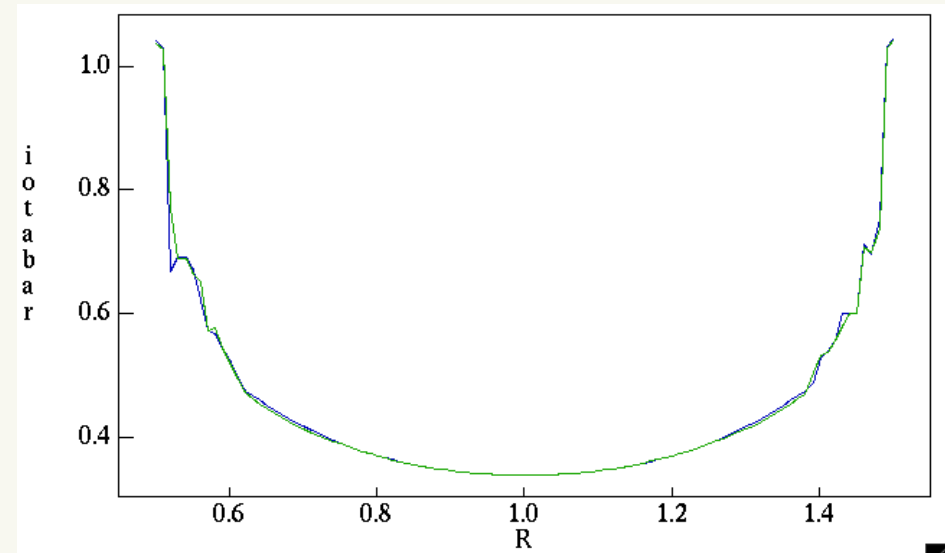


Figure 18: Rotational transform profiles at $t=0$ and $t=4.8 \cdot 10^{-4}$ s.

The helically symmetric ($m=2, n=2, \epsilon=.75$) case is perturbed and heated.

As β increases, stochastic regions start at the edge of the plasma and grow inward. Shortly thereafter, the simulation halts.

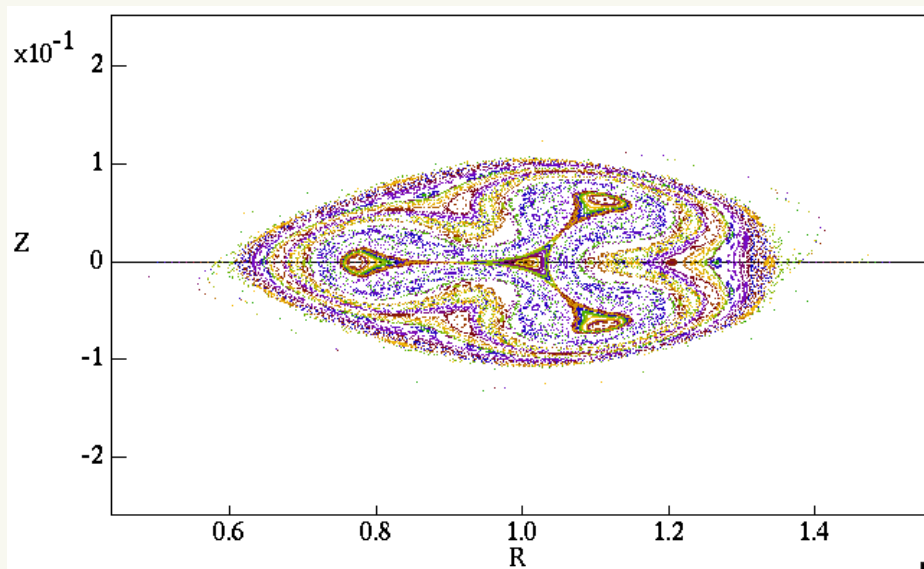


Figure 19: Poincaré plot at $t=9.2 \cdot 10^{-4} \text{ s}$, $\zeta = 0$.

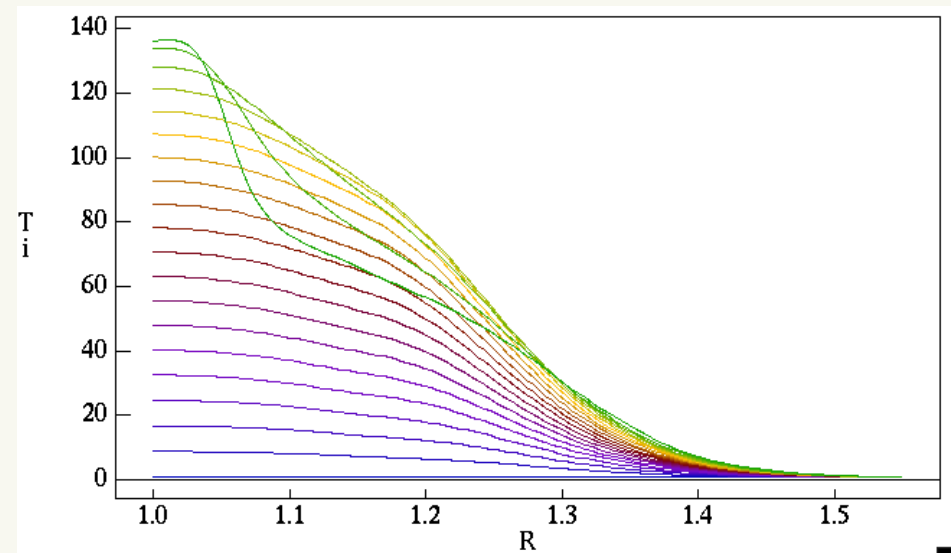


Figure 20: Temperature profile at various times.

The perturbed helically symmetric ($m=2, n=2, \epsilon=.75$) case see the onset of instability at $\beta \sim 1\%$.

$n=1$ and $n=3$ modes grow large and destroy the plasma.

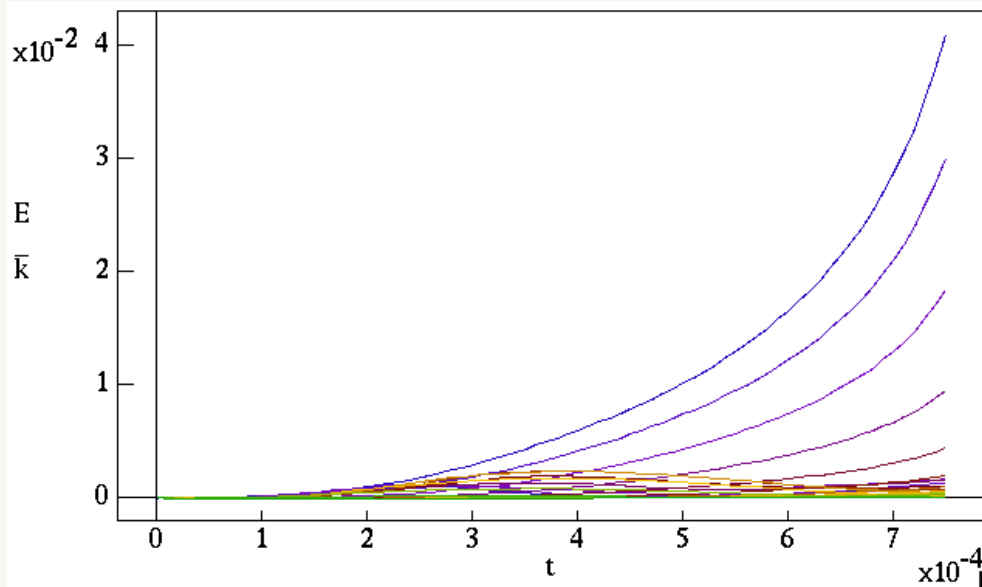


Figure 21: Kinetic energy for all modes.

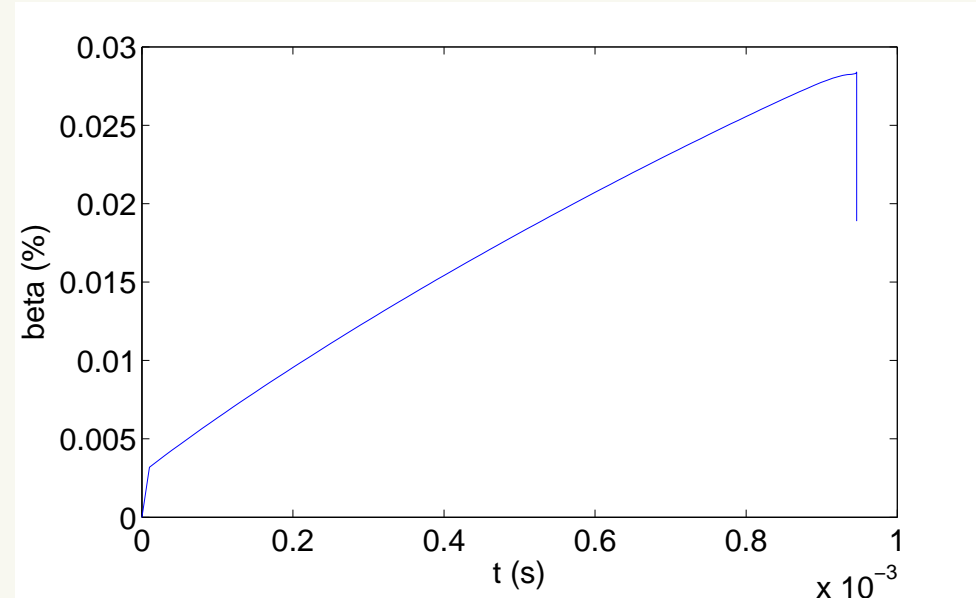


Figure 22: Maximum $\beta=2.84\%$.

The spoiled symmetry ($m=2, n=2, \epsilon=.75$) case is perturbed and heated (Case 2).

This time, small changes are noticed in the flux surfaces - some stochasticity in the edge, as well as subtle changes in the core.

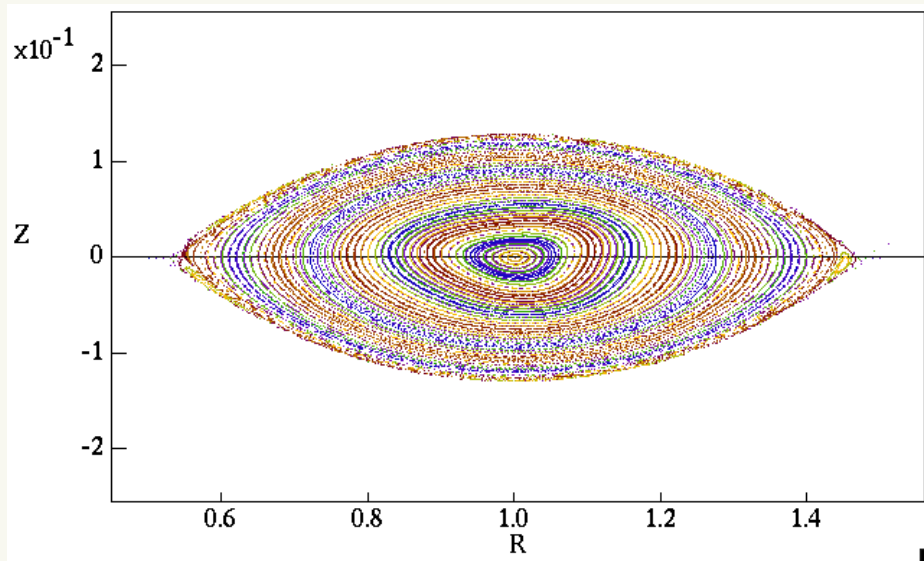


Figure 23: Poincare plot at $t=1.00 \cdot 10^{-3}$ s, $\zeta = 0$.

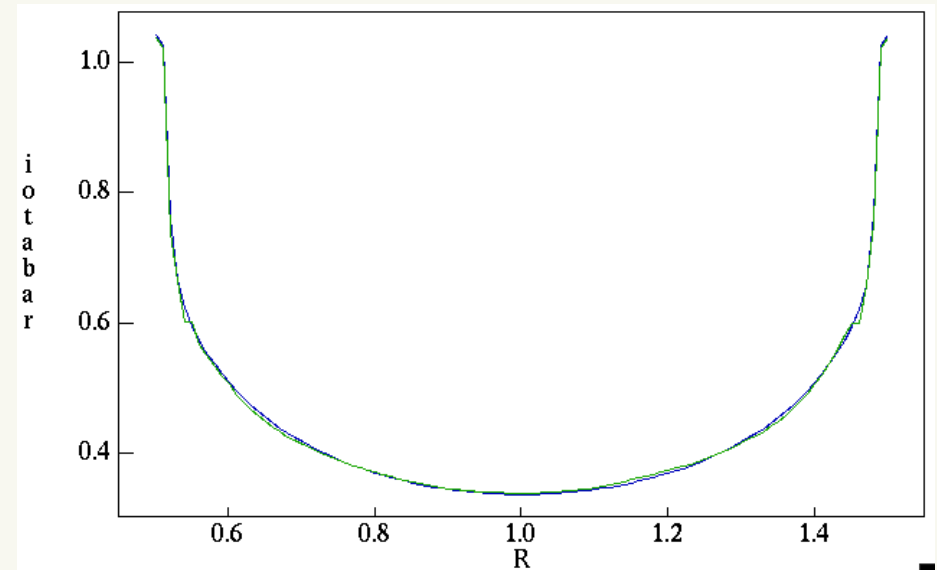


Figure 24: Rotational transform profiles at $t=0$ and $t=1.00 \cdot 10^{-3}$ s.

The spoiled symmetry ($m=2, n=2, \epsilon=.75$) case is perturbed and heated.

As β increases, the stochastic edge region grows and changes are seen in the core structure. Shortly thereafter, the simulation halts.

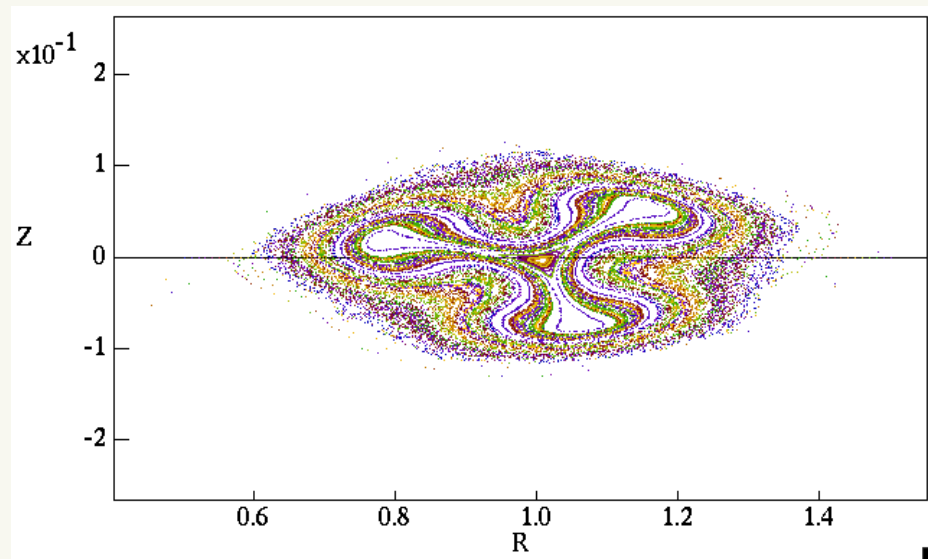


Figure 25: Poincaré plot at $t=1.18 \cdot 10^{-3}$ s, $\zeta = 0$.

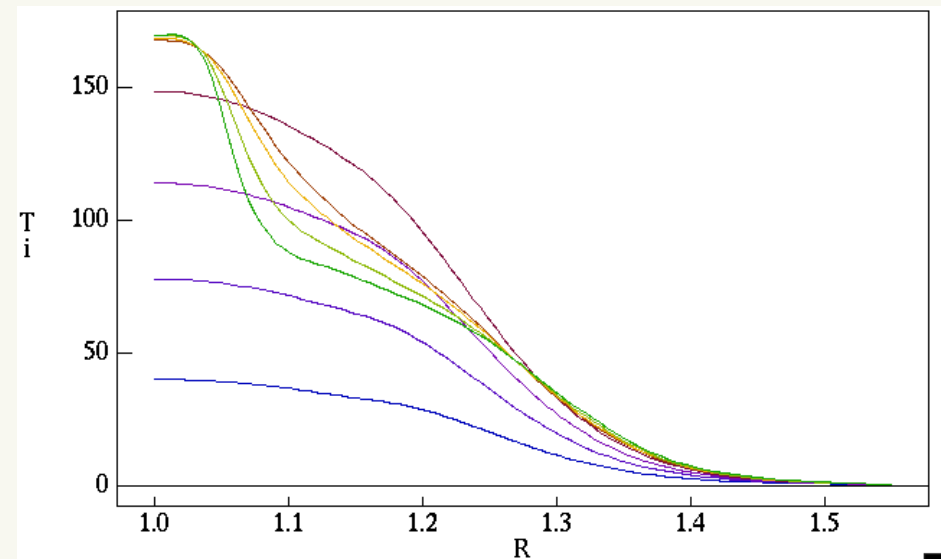


Figure 26: Temperature profile at various times.

The spoiled symmetry ($m=2, n=2, \epsilon=.75$) case sees the onset of instability at $\beta \sim 3\%$.

$n=1$ and $n=3$ modes grow large and destroy the plasma.

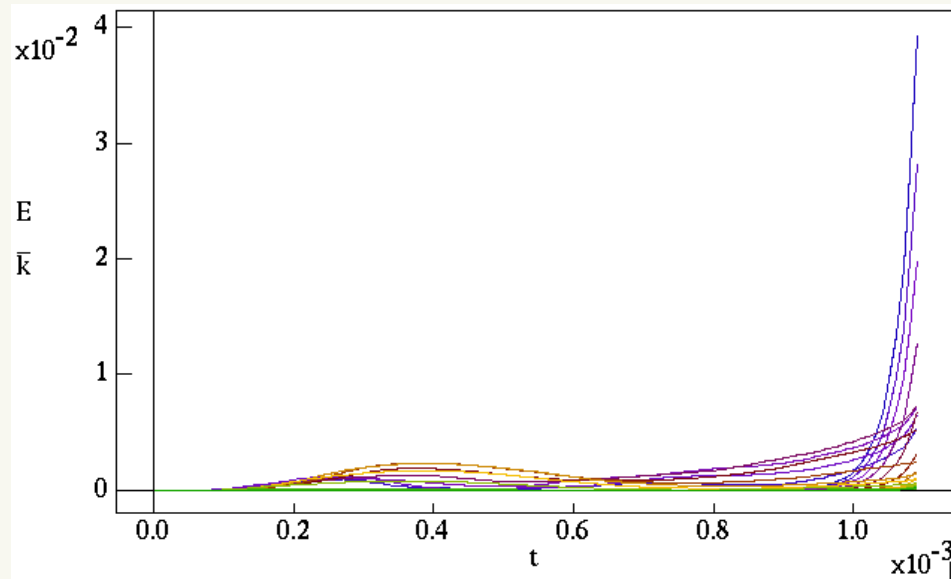


Figure 27: Kinetic energy for all modes.

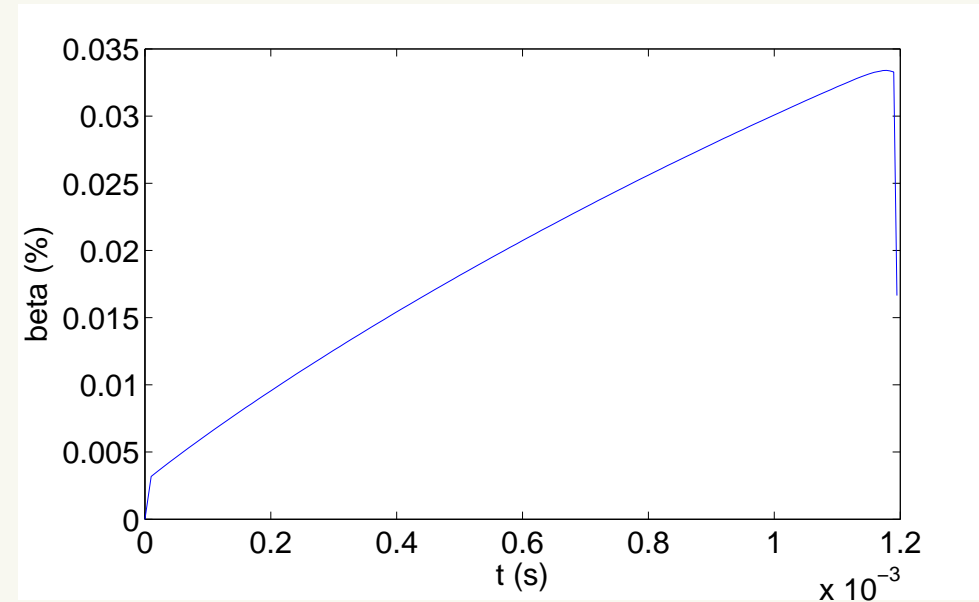


Figure 28: Maximum $\beta=3.34\%$.

Summary of these simulations:

For the slow heating cases:

- A resistive core mode appears in both the helically symmetric case and the spoiled-symmetry case.
- Both cases reach the same peak value of beta: 1.05%.

=> The presence of the stochastic edge seems to have no effect on the onset of this mode.

For the fast heating cases:

- Onset of MHD activity in the edge is delayed in the spoiled symmetry case.
- Onset β of the edge modes is higher in the spoiled symmetry case. ($\sim 1\%$ vs. $\sim 3\%$).
- In some cases, the spoiled symmetry vacuum configuration actually achieves *higher* β than the *unperturbed* vacuum helically symmetric case.

Possible explanation of this phenomenon.

Small stochastic field at the edge acts to limit the pressure gradient that can build. Note that a pressure gradient **does indeed exist** in the **stochastic** region.

- Limits the drive for an interchange instability. A kind of safety valve, so that too much pressure doesn't build.
 - Appears to prevent the onset of edge localized modes.
- However, this stochasticity does not affect the formation of core modes.

Future Work.

- Further explore the possible combinations:
 - Vacuum magnetic field - to date have only looked at $\epsilon = .75$, $\epsilon = .85$, $\epsilon = .87$, with dominant 2,2 harmonics.
 - Heating scheme - to date have only investigated 2 heating rates with a linear profile from center to edge of plasma
 - Degree of anisotropic heat conduction - to date have only used $\chi_{\parallel}/\chi_{\perp} = 10^6$.
- Identify the mode structure of the instabilities.
 - Code has been written which analyzes the harmonic structure of the Pfirsch-Schlüter spectrum in helical space.
 - Code is being developed that analyzes $\mathbf{v} \cdot \nabla\psi$ and $\mathbf{b} \cdot \nabla\psi$.
- Perform a β -scan, where the critical β which triggers instability is accurately determined for these cases.
- Adjust χ_{\parallel} to investigate the effect of varying the allowable pressure gradient that the stochastic region can support.